Thin–Walled Structures 151 (2020) 106740

Contents lists available at ScienceDirect

Thin-Walled Structures

journal homepage: http://www.elsevier.com/locate/tws

Full length article

Optimal structural design searching algorithm for cooling towers based on typical adverse wind load patterns

Lin Zhao [a,b,c], Wei Cui [a,b,c,*], Yanyan Zhan [b], Zhinan Wang [b], Yuwen Liang [b], Yaojun Ge [a,b,c]

[a] State Key Lab of Disaster Reduction in Civil Engineering, Tongji University, Shanghai, 200092, China
[b] Department of Bridge Engineering, College of Civil Engineering, Tongji University, Shanghai, 200092, China
[c] Key Laboratory of Transport Industry of Bridge Wind Resistance Technologies, Tongji University, Shanghai, 200092, China

ARTICLE INFO

Keywords:
Large cooling tower
Wind tunnel test
Interference criteria
Adverse load pattern
Structural optimization

ABSTRACT

This investigation aims at typical adverse wind load patterns under tower group interference and overall structure optimization of large cooling towers considering multiple geometric parameters, focusing on potential unfavorable load patterns. Wind tunnel tests were performed on typical six-tower groups with various central distances, incoming flow directions and arrangement types, and external wind pressures were measured under interference conditions. Adverse wind load patterns are summarized with the help of interference criteria for three parameters: aerodynamic load, structure response and weighted internal force combination. Furthermore, overall structure optimization is achieved through the hybrid of grid search and gradient descent method, taking into account various possible wind loading distributions. Total 13 geometric parameters are adjusted to seek an optimized design that satisfy the requirement of structure strength, stability and economy under a particular wind load pattern. Crossover checks are then introduced to select a final optimized design scheme that is universally applicable to different adverse wind load patterns. The optimization procedure proposed in this study shows that adverse wind load patterns of grouped towers has distinct features comparing with wind load codes. It is necessary to consider the influence of multiple typical adverse wind load patterns for structural design, and the final optimization scheme should be determined through crossover checks to guarantee structure safety, stability and economy of cooling towers.

1. Introduction

As the increasing huge demand for electric power, a large amount of cooling towers with limit-breaking heights and grouped cooling towers with complex arrangements have been built and under construction in mainland of China [1]. Consequently, complex groups of high-rise cooling towers with high density arrangement become more sensitive to wind effects [2], and it is necessary to deeply understand the adverse wind load patterns under complex group tower arrangements. On the other hands, because of the great construction volume, it is also important to optimize the structural design, prolong the service life [3,4] and reduce construction cost. The ultimate goal is to achieve the balance between structural safety and financial cost from the point view of performance-based wind engineering [5,6].

Wind interference effect on the cooling towers caused by surrounding buildings and terrains is still a popular research topic. A series of field measurements [7–14] and wind tunnel tests [15,16] have been implemented since the collapse of the Ferrybridge cooling towers [17] in 1965. Simplified 2-D static wind pressure curves around tower shells have been proposed and have been widely accepted for several decades. However, these curves are not sufficient when being applied to more complex grouped-tower combinations, especially when the number of grouped towers and their heights are beyond the conventional limit [18,19].

It is necessary to reevaluate the current wind load patterns specified by national load Codes [20–22] and to compare with the wind load patterns for super tall and complex grouped cooling towers derived from wind tunnel tests. Small geometrical optimization can lead to significant deviations in structural response of cooling towers [23]. There are several key points in cooling tower design process including adjustable variables, multiple design targets, optimization algorithms and wind load patterns. Depending on the number of variables, single and multiple parameters optimization may be used. The former is usually realized by univariate comparison and parameter sensitivity analysis, which

* Corresponding author. 207 Wind Engineering Building, Tongji University, 1239 Siping Road, Shanghai, 200092, China.
E-mail address: cuiwei@tongji.edu.cn (W. Cui).

https://doi.org/10.1016/j.tws.2020.106740
Received 16 October 2019; Received in revised form 15 February 2020; Accepted 18 March 2020
Available online 8 April 2020

can identify the sensitivities of individual parameters, involving ring stiffeners [24–26], shell height [27], shell thickness [28], shell radius [29], meridian line [28,30], angles of air inlet [31] and etc. The current structural optimization of high-rise buildings are either for overall structural dynamic properties [32], such as stiffness, or aerodynamic shape optimization [33]. When the number of variables is large, multi-parameter optimization is necessary, and high-efficiency optimization methods are required due to the large amount of time-consuming computation. For the optimization target, the existing criteria are quite diverse, which include construction cost [27], membrane stress [28,29], shell mass [34], stability [31], ultimate bearing capacity [30] and etc. The variety of optimization targets makes it challenging to consider them simultaneously. Some investigations on cooling tower optimization mentioned above are listed in Table 1.

Currently, in the field of wind effects on super tall and complex grouped cooling towers, the following problems still exist. First of all, a unified optimization framework has not yet been setup. The above mentioned literature considered either structure response (internal force or displacement) or economic efficiency as target functions separately. Thus, it is required to clearly define to the structural design restriction (optimization constraints) and unify all construction cost as the optimization objects. Secondly, several widely-used optimization methods only consider the upper tower shell only, and substructure as the foundation to the whole structure is normally neglected. At last, the variety of wind load patterns due to increasing tower height and complex towers arrangement was often ignored, and most existing engineering practice is still limited to symmetrical 2-D wind pressure simplified from an isolated tower.

Due to these issues, this study focuses on typical adverse wind load patterns under complex interference and overall structure deign optimization algorithm. This following research will have two parts. The first parts focuses on typical adverse wind load patterns from a large number of wind pressure measurement from wind tunnel tests due to grouped towers interference effects. According to experimental results, typical adverse wind load patterns are examined according to comprehensive evaluation criteria for three parameters: wind load, structure response and weighted internal force combinations [18].

The second part presents a structural design optimization framework for a series of proposed adverse wind load patterns, which includes two steps. Step 1 is structural design parameter optimization for each adverse wind load pattern. This was achieved through a hybrid optimization algorithm combining grid search method [37] and gradient descent method [38]. Step 2 is a crossover check that examine several wind load patterns effects on optimized structural design obtained from step 1. Finally, one optimized structural design scheme with lowest construction cost is selected, which also can satisfy all design requirements. The whole process is shown in Fig. 1. To illustrate the application and process of these structural framework, a case study of a six-tower combination is carried out in following sections.

Table 1
Representative investigations on cooling tower optimization.

Literature	Variables	Targets	Algorithm	Restrictions
Böhm (1960) [27]	Shell height	Material cost		Buckling factor
McLone (1963) [29]	Shell radius	Membrane stress		Buckling factor
Croll (1969) [28]	Meridian line	Membrane stress		Buckling factor
Croll (1971) [34]	Shell thickness	Shell mass, stability		Buckling factor
Greiner-Mai (1972) [30]	Meridian line	Ultimate capacity, construction cost		Buckling factor
Noh (2006) [31]	angle of air inlet	Stability, material consumption		Buckling factor
Uysal et al. (2007) [35]	Multiple geometry variables	Shell mass	Linear Programming	Buckling, von-Mises stress
Lagaros et al. (2006) [36]	Multiple geometry variables	Shell mass	Evolution algorithm	Buckling, Uniaxial and tri-axial stress

2. Typical adverse wind load patterns from wind tunnel experiments

2.1. Wind tunnel test

Pressure measurement tests on rigid cooling tower models were performed to collect wind pressures distribution characteristics with complex interference conditions. The tests were carried out in an atmospheric boundary layer wind tunnel, and testing section dimension is 15 m wide, 2.0 m high and 14 m long. Spires and roughness blocks were applied to simulate wind boundary profile and turbulence characteristics of open terrain ($z_0 = 0.3$ m). Pressure measurement tests with rigid models were performed to collect wind pressures under complex interference conditions. Detailed information can be refereed to Refs. [18].

The height of prototype cooling tower is 250 m, which will be tallest cooling tower and used as one part of proposed nuclear power plant project. Its main dimensions are illustrated in Fig. 2a).

Considering blockage ratio restriction and Reynolds number effects, a geometric scale of 1:200 was adopted. There were $12 \times 36 = 432$ pressure taps installed on the external surface of the shell (12 layers along the meridian, 36 taps arranged evenly in every layer), as shown in Fig. 2 b). The location of pressure taps are defined as circumferencial angle θ starting from wind direction ϕ, which is defined in Fig. 4a). There was no tap on the internal side of the shell since internal wind pressure is steady compared with external ones [39]. In this study, the internal wind pressure coefficient was set as -0.5 according to Chinese cooling tower design Code [40].

In the following content, wind pressure coefficient C_p thereafter refers to external ones unless specified differently. To compensate the Reynolds number effects, 36 paper tapes (12 mm wide and 0.1 mm thick, stretched from top to bottom) were pasted uniformly around the circumference. Through adjustment of surface roughness and incoming wind speed, the average pressure coefficient C_p (Fig. 3) were coincident with values from the Chinese Code [40] and the fluctuating RMS pressure coefficient σ_{C_p} were also comparable against previous field measurement [14].

Combinations of tower group arrangement L/D (L: center-to-center distance between adjacent towers; D: base diameter of structure) and incoming flow direction ϕ create a rich and varied number of test cases, as listed in Table 2.

As shown in Figs 4 and 5, six grouped tower with rectangle (Rec) and rhombus (Rho) arrangements were selected according to present engineering practice and design Codes. The Six-towers arrangement are used widly in power plant porjects and can be easily reduced to 2, 3 and 4 tower combination, or reorganized to 8 and 12 tower combination. The wind loading results of six-tower arrangement can be used as reference value (may not the exact value) for initial design of other numbers tower arrangement. L/D values were set as 1.5, 1.75 and 2.0 and incoming wind direction ϕ (defined in Fig. 4) ranged from 0° to 360° in increments of 22.5°. Measured towers are marked in Fig. 4, and represent all the possible interference cases due to geometric symmetry of arrangement forms.

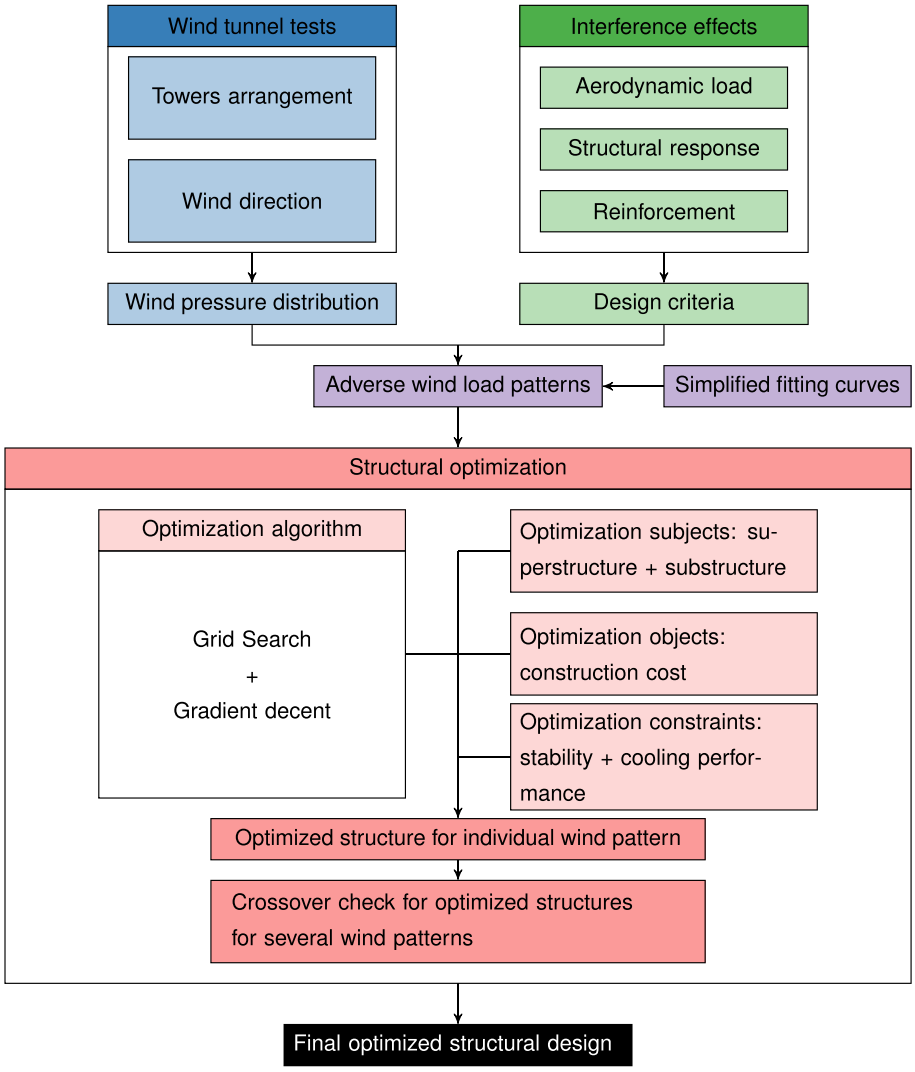

Fig. 1. Flow chart of cooling tower structural design optimization framework.

2.2. Selection of adverse wind load patterns

Predominant adverse wind load patterns (WLPs) are selected to reflect the most unfavorable loading effects so that other possible interference conditions can be covered. Interference factor (IF) is widely employed to evaluate surrounding structures interference wind effects. However, it is still debatable for the selection of IF criteria because of varieties of wind loads and wind effects including wind-induced external loads, internal force, internal stress and structural performance for various parts of the whole towers. The evaluation of interference wind effect for those different perspectives may not consistent due to the complexity of interference effects and structural mechanical properties.

Therefore, previous study [18] summarized 25 different IF criterias including different aspects of wind effects on structures to reflect both serviceability and ultimate limit states of cooling towers.

For the above mentioned 241 (1 + 96+144) wind tunnel tests configurations, there are some potential possible "maximum" cases for each group IFs, and the corresponding condition is defined as the adverse WLP.

Frequency distribution of adverse WLP for all each IFs is counted in Fig. 6 [18], where proportions of Rec and Rho were 12% and 88%, respectively, which shows obvious worse wind effect of the latter arrangement. In Fig. 6, larger IF generally occurs in similar testing configurations, which will be detailedly discussed in the following subsection. Among the 25 adverse cases, Rho_1.75L/D_T1 appears most frequently: 9 times in total, and its most unfavorable wind direction ϕ is 315°, which appears 8 times. Then the second worst configurations is Rho_1.5L/D_T2, appearing 4 times, whose unfavorable ϕ is 90°.

Other configurations do not appear very frequent. As a result, the average C_p of Rho_1.75L/D_T1_315° and Rho_1.5L/D_T2_90° are proposed as the typical adverse WLPs. Additionally, single tower and Rec_1.5L/D_T1_0° are also employed according present Chinese cooling tower design Code [40].

2.3. Characteristic of typical wind load patterns

Wind pressure coefficients, C_ps, of all four previously selected tower arrangement configurations are shown in Fig. 7 and their characteristics will be discussed in detail in this section.

2.3.1. Code-specified symmetrical 2-D wind load pattern for isolated tower

C_p distribution of a single tower are plotted in Fig. 7a). Because the model is symmetric and isolated, the C_p from test measurement is also symmetric and consistent with the coded value in Refs. [40].

Taking incoming flow direction as the symmetric axis, C_ps distribute symmetrically and can be divided into 3 areas: windward area

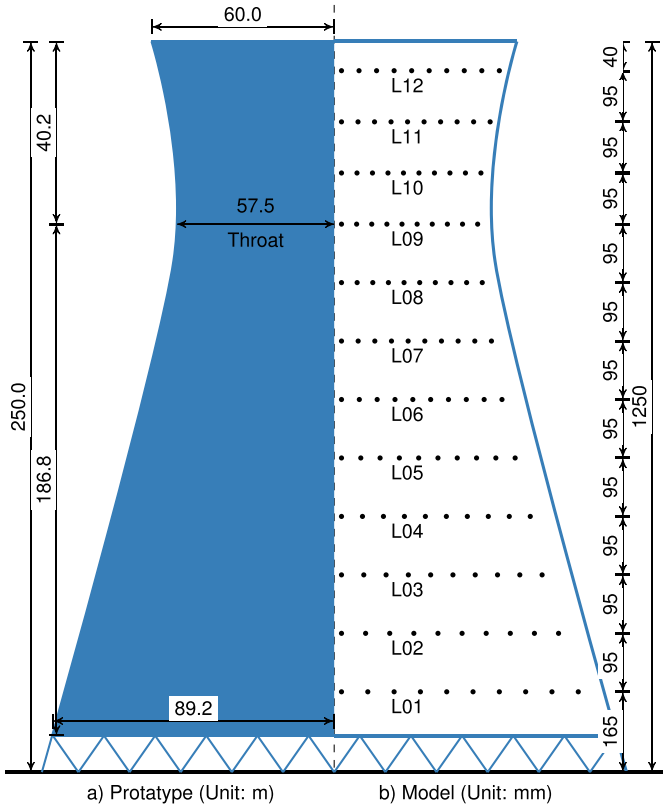

Fig. 2. Cooling tower dimensions and pressure tap arrangement.

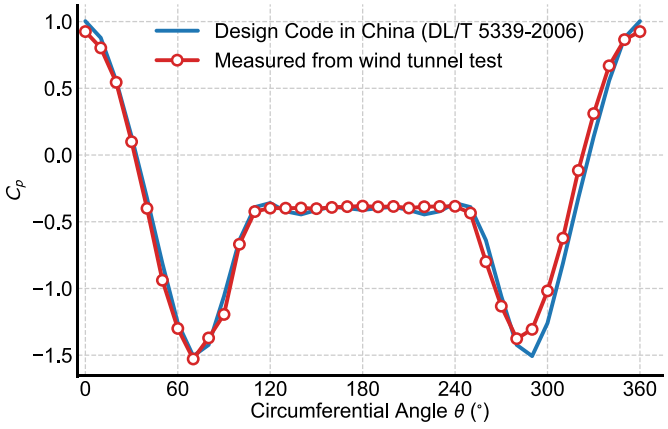

Fig. 3. Average wind pressure coefficient simulation.

Table 2
Summary of test cases.

Arrangement	L/D	Measured tower	Number of ϕ	Total case number
Single Tower	N/A	N/A	1	1
Rec	1.5, 1.75, 2.0	T1, T2	16	96 (3 × 2 × 16)
Rho	1.5, 1.75, 2.0	T1, T2, T3	16	144 (3 × 3 × 16)

(330°–30°), lateral wind area (30°–120°, 240°–330°) and leeward area (120°–240°). In the windward area, C_ps are positive and the maximums appear at the symmetric axis, then C_ps decrease dramatically along both direction.

In the lateral wind area, C_ps are negative, and their maximums appear at 70° and 290° symmetrically. In the leeward area, C_ps are negative and steady around −0.5. Generally, C_ps distribution of the single tower agrees well with the Chinese Code with the exception of lateral wind and leeward area near the shell top and bottom. This pattern is named as Code-specified symmetrical 2-D wind load pattern (C–S-2D) in the remaining content.

2.3.2. *Shelter-controlled asymmetrical 3-D wind load pattern*

C_p distribution of Rec_1.5L/D_T1_0° case is shown in Fig. 7b), which shows two obvious characteristics. First, C_ps are obviously smaller than Code values in Ref. [40]. This overall reduction is because of "shielding effect" provided by surrounding towers. Additionally, since the tower dimension varies along height, the "shielding effect" also changes at different pressure taps levels, which is different than symmetric single tower and called 3-D features in this study.

Second, there is clear asymmetry in windward and lateral area, which is due to asymmetrical surroundings tower arrangement. When the flow comes from 0°, the left side of T1 is directly exposed to winds, while the right side has surroundings towers. Neighboring towers lead to airflow acceleration due to "funneling effect", which changes local wind pressure distribution. In summary, "shielding effect" plays a dominate role and "funneling effect" is subordinate for this wind load pattern. It should be noted that asymmetrical C_p may is more unfavorable for structural safety than C–S-2D even though the absolute values are smaller. Considering its characteristics, this wind load pattern is called shelter controlled asymmetrical 3-D wind load pattern (S-A-3D).

2.3.3. *Funneling-controlled asymmetrical 3-D wind load pattern*

distribution of Rho_1.75L/D_T1_315° is shown in Fig. 7c). Comparing with single tower case, C_p peak value is a little larger, and the peak appears at left lateral wind area. Furthermore, asymmetry in lateral wind area and leeward area is obvious, because of the "funneling effect" offered by T2. This wind load distribution pattern is named Funneling controlled asymmetrical 3-D wind pressure (F-A-3D).

2.3.4. *Funneling-controlled symmetrical 3-D wind load pattern*

For Rho_1.5L/D_T2_90°, C_ps are generally symmetrical besides little local asymmetry in lateral wind area, which is shown in Fig. 7d). When flow comes from 90°, surrounding interference on T2 is generally symmetrical. Compared with the Code, maximal absolute values are larger in lateral and leeward areas. This phenomenon is caused by "funneling effect": when the air flow passes a funnel formed by the front towers located in the incoming flow directions, and wind speed is consequently accelerated. The wind load pattern is defined as funneling controlled symmetrical 3-D wind pressure (F–S-3D).

2.4. *Summary of wind load patterns*

Wind load patterns and corresponding test conditions are summarized in Table 3. For convenience, they are referred to hereafter by corresponding abbreviations or pattern numbers.

Design wind load is expected to be elegant for the seek of the convenient engineering application. Therefore, it is necessary to describe adverse wind load patterns through a concise formula. The fitting here only focuses on the latter 3 wind load patterns since single tower test results agrees well with the Code. Due to gradual change of C_p from the cooling tower bottom to the top, the whole shell is divided into 3 parts along the shell height H: lower part ($\leq 0.3H$), middle part ($0.3H \sim 0.8H$) and upper part ($\geq 0.8H$). To keep in line with the common design practice and specification, Fourier expansion with 8 order is employed as the fitting formula as in Eq. (1). Fitted parameters are listed in Table 4. Fig. 8 displays the fitted curves of the four typical WLPs. Compared with the Code, there are obvious differences in the fitting curves, but they are comparable with the tests results in Fig. 7 and can be

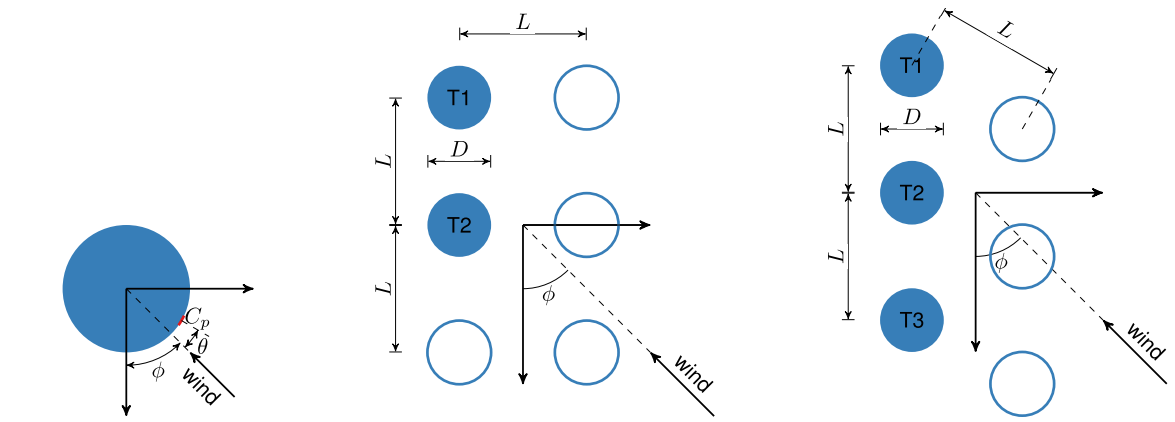

(a) Wind direction definition **(b)** Rectangle arrangement **(c)** Rhombus arrangements

Fig. 4. Six-tower arrangements and incoming flow direction.

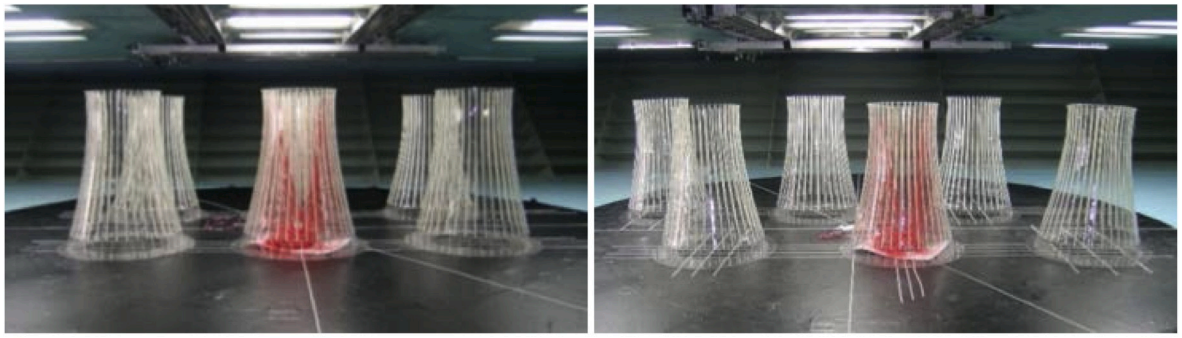

(a) Rectangle arrangement **(b)** Rhombus arrangements

Fig. 5. Six-tower arrangements in wind tunnel.

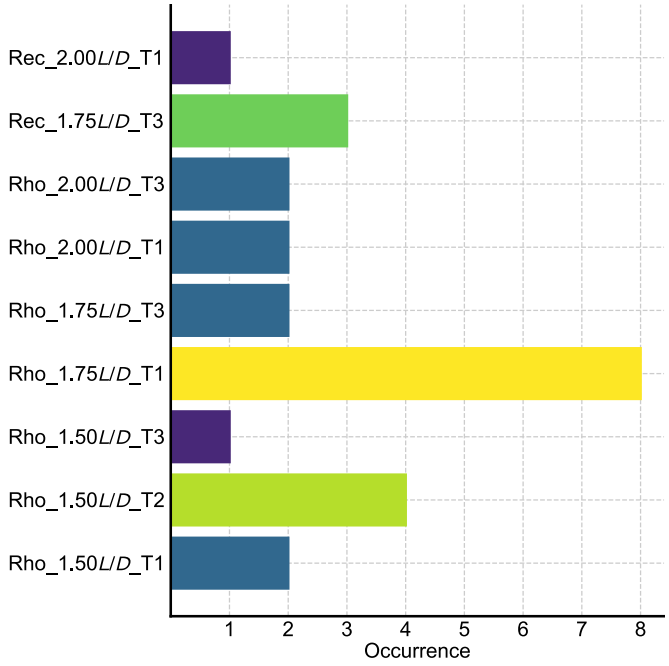

Fig. 6. Frequency distribution of most adverse cases [18].

used as wind loads for structural design and optimization in later stage.

3. Structural optimization methodology

3.1. Structural optimization description

Optimization of structural design for cooling tower is a step-by-step searching algorithm of structural geometry shapes and dimensions, aiming to identify the most economic design parameter with least construction material resources. During the optimization process, the material (concrete and steel reinforcement) strength, overall and local structural stability are considered as the constraints.

3.1.1. Optimization variables

In this study, total 13 cooling tower geometry parameters are chosen

Table 3
Typical adverse wind load patterns and their characteristics.

$$C_p(\theta) = \sum_{i=0}^{7}[a_i\cos(i\theta) + b_i\sin(i\theta)] \quad (1)$$

Pattern No.	Pattern name	Tower Arrangement	Symmetry	Comparison against the Code
WLP1	C–S-2D	Single	Symmetric	Similar
WLP2	S-A-3D	Rec_1.5L/D_T1_0°	Asymmetric	Reduced
WLP3	F-A-3D	Rho_1.75L/D_T1_315°	Asymmetric	Amplified
WLP4	F–S-3D	Rho_1.5L/D_T1_90°	Symmetric	Amplified

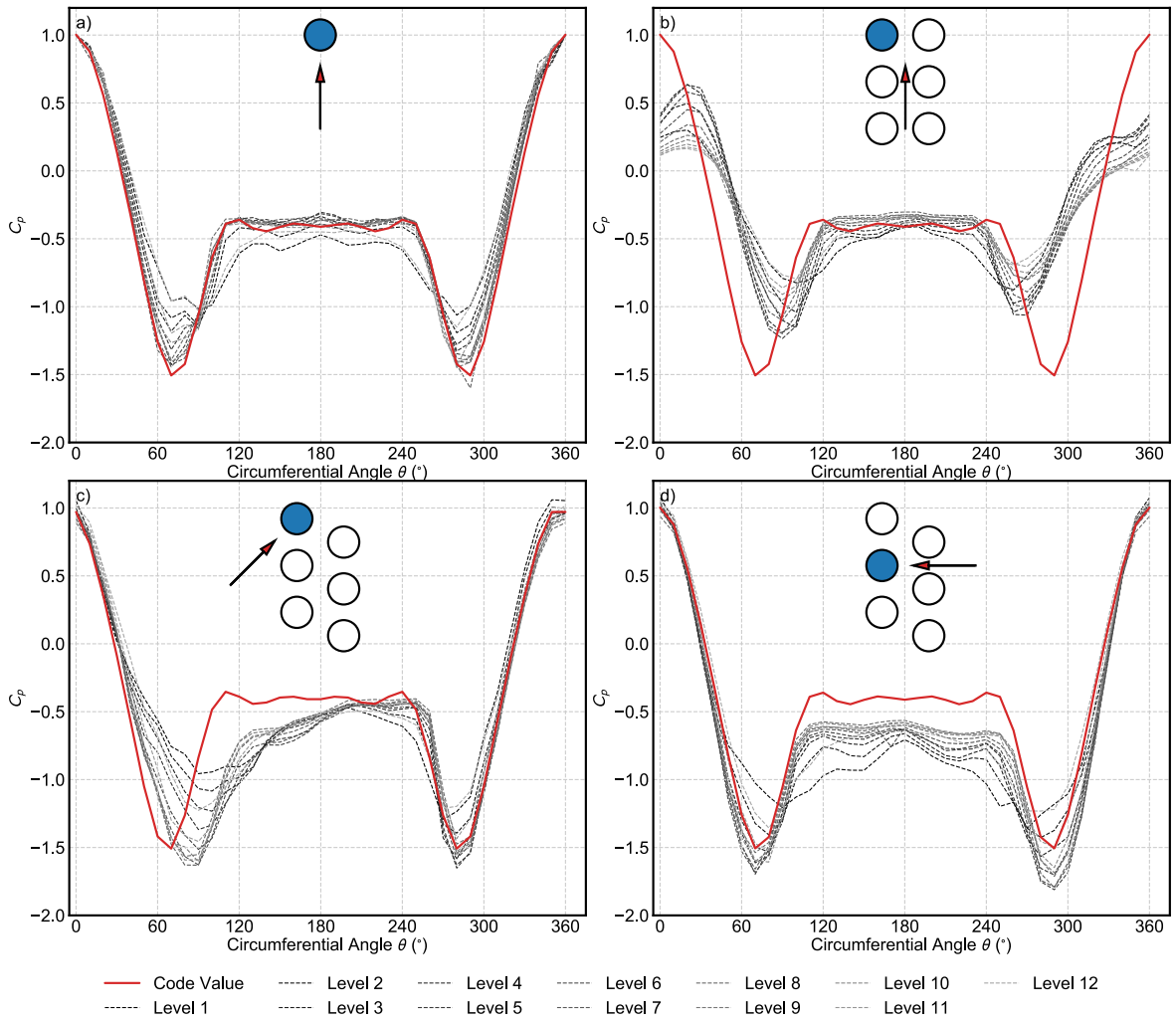

Fig. 7. Average C_p of four typical WLPs.

as optimization variables. The heights and diameters of tower components are fixed due to the thermal engineering considerations, and they are excluded from the optimization variables and denoted as Capitalized variables. 13 cooling tower geometry parameters are illustrated in Fig. 9.

The cooling tower shell thickness $t(z)$ changes gradually according to Eq. (2) along the meridional height, which are controlled by 5 key parameters:top thickness t_1, throat thickness t_2, bottom thickness t_3, the upper part thickness variation coefficient α_1 and lower part thickness variation coefficient α_2.

$$t(z) = \begin{cases} t_2 + (t_1 - t_2)\exp\left(-\alpha_1 \dfrac{H_1 - z}{R_2}\right) & h \geq 0.75H_1 \\ t_2 + (t_3 - t_2)\exp\left(-\alpha_2 \dfrac{z - H_4}{R_2}\right) & h \leq 0.75H_1 \end{cases} \tag{2}$$

Among them, θ_1 and θ_2 greatly influence the shape of the shell meridian; t_2 is critical to structural stability; t_3 bounds the range of t_1 and t_2; and the ellipse supporting pillars' size: l_1, l_2 and base ring's size: l_3 and l_4 have significant influence for overall structural stiffness of cooling tower's substructure.

Because of construction feasibility, the geometry parameters are normally not continuous variables, each parameter's upper and lower limit and increment requirement are listed in Table 5.

3.1.2. Optimization constraints

Due to the cooling tower internal thermal mechanics and cooling efficiency, the optimization variables mentioned above, the outlet angle θ_1 and inlet angle θ_2 have specific requirement:

$$\tan\theta_1 > \frac{R_1 - R_2}{H_1 - H_2} \tag{3}$$

$$\tan\theta_2 > \frac{R_3 - R_2}{H_2 - H_4} \tag{4}$$

Also, because of construction feasibility, the outlet angle θ_1 and inlet angle θ_2 and inlet tower shell thickness t_1 are bounded as:

$$7^\circ \leq \theta_1 \leq 9^\circ \tag{5}$$

$$13^\circ \leq \theta_2 \leq 21^\circ \tag{6}$$

$$t_2 \geq 0.25 \text{ m} \tag{7}$$

Besides the geometry limitation, the cooling tower throat diameter and top thickness should satisfy the overall structural stability requirement from Chinese design Code [40], which is shown in Eq. (8).

$$\lambda_g = \frac{0.052E_c\left(\frac{t_1}{R_2}\right)^{2.3}}{\gamma_w \beta \frac{1}{2}\rho V_{H1}^2 C_{p,H_1}} \geq 5 \tag{8}$$

where λ_g is global stability factor, E_c is the concrete Yang's modulars, γ_w is the wind loads partially coefficient, β is the turbulence coefficient depending on ground roughness, ρ is air density, V_{H1} is the design wind

Table 4
Typical adverse wind load patterns and their characteristics.

WLP	Code	S-A-3D			F-A-3D			F–S-3D		
Part	N/A	Lower	Middle	Upper	Lower	Middle	Upper	Lower	Middle	Upper
a0	−0.443	−0.340	−0.349	−0.340	−0.659	−0.651	−0.572	−0.452	−0.535	−0.477
a1	0.245	0.401	0.261	0.234	0.466	0.310	0.400	0.479	0.380	0.440
a2	0.675	0.416	0.428	0.306	0.678	0.721	0.694	0.651	0.720	0.696
a3	0.536	−0.013	0.064	0.018	0.395	0.573	0.460	0.268	0.415	0.337
a4	0.062	−0.157	−0.184	−0.107	0.114	0.133	0.069	0.016	−0.017	−0.030
a5	−0.138	−0.014	−0.051	−0.013	−0.007	−0.102	−0.072	−0.014	−0.087	−0.069
a6	0.001	0.043	0.061	0.023	0.058	−0.015	0.020	0.034	0.017	0.034
a7	0.065	−0.018	0.005	−0.009	0.003	0.028	0.047	0.041	0.037	0.045
b1	0	−0.017	−0.018	−0.010	0.061	0.062	0.019	−0.047	−0.157	−0.139
b2	0	0.015	0.034	0.033	0.006	0.002	0.004	0.072	0.079	0.063
b3	0	0.023	0.080	0.053	−0.007	−0.008	0.020	−0.121	−0.013	−0.006
b4	0	0.035	0.062	0.026	0.000	−0.015	0.016	−0.143	−0.094	−0.080
b5	0	0.015	0.001	−0.007	−0.009	−0.009	−0.001	−0.003	−0.044	−0.023
b6	0	0.012	−0.010	−0.003	−0.018	−0.008	−0.009	0.031	0.064	0.042
b7	0	0.010	0.005	0.005	0.000	−0.004	−0.006	−0.021	0.015	0.012

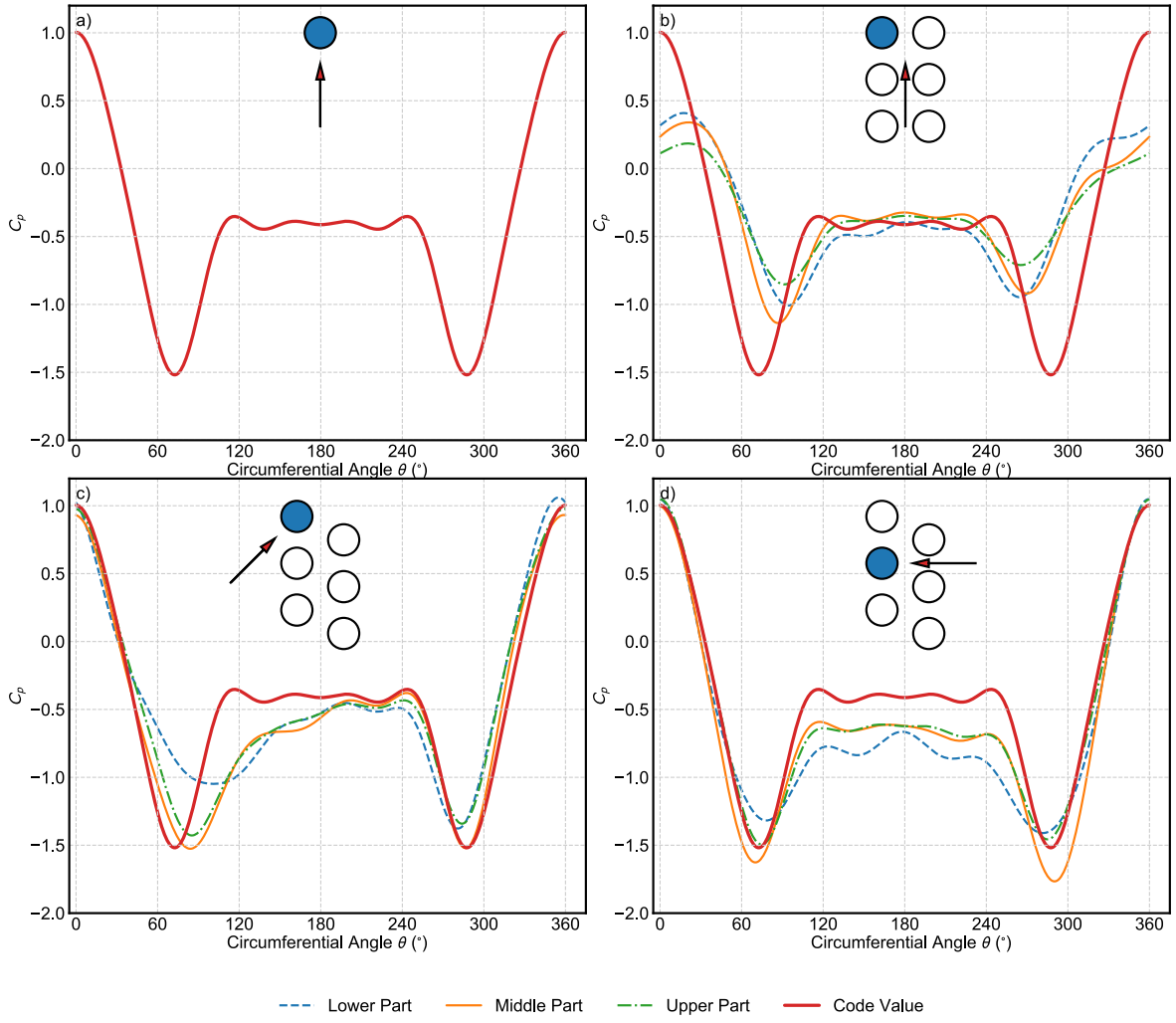

Fig. 8. Four typical WLPs fitted by Eq.(1)

speeds at cooling tower top of 50 year return period and C_{p,H_1} is the mean wind pressure coefficient at cooling tower top determined by wind tunnel test. According to Ref. [40], γ_w is 1.4 and β is 1.9 for ground roughness as open terrain. $\frac{1}{2}\rho V_{10m}^2$ is the basic wind pressure at 10 m height, and assumed as 0.5 kPa (basic wind speeds is 28 m/s) in this study.

3.1.3. Optimization target

The construction material cost C in terms of concrete volume V_c and steel weight M_s consumed is selected as the optimization target:

$$C = V_c P_c + M_s P_s \tag{9}$$

where P_c and P_s are the unit price for concrete and steel, respectively, and P_c is assumed as 500 local currency per cubic meter and P_s is

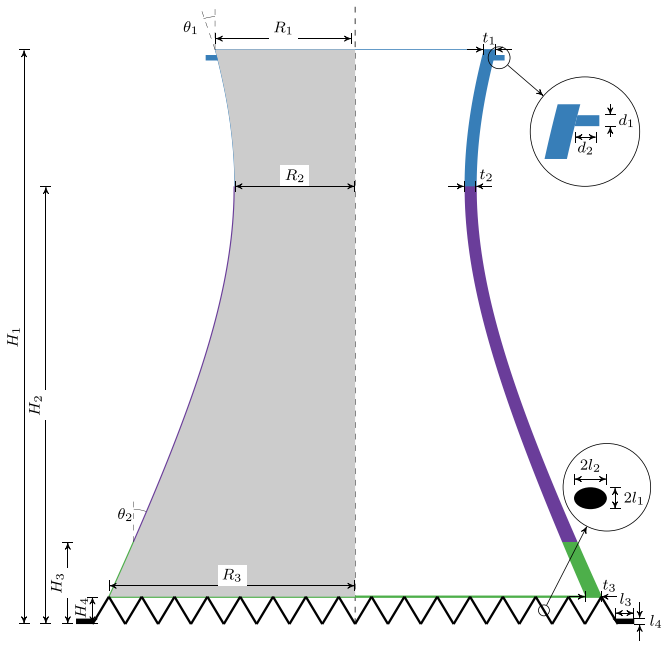

Fig. 9. Optimization Geometric parameters.

Table 5
Limitations for cooling tower structural optimization.

Variables	Limits	Increment	Variables	Limits	Increment
θ_1 (°)	[7,9]	1	θ_2 (°)	[13,21]	1
d_1 (m)	[0.2, 0.6]	0.1	d_2 (m)	[0.9, 1.5]	0.1
l_1 (m)	[0.6, 1.2]	0.1	l_2 (m)	[0.6, 1.2]	0.1
l_3 (m)	[6.0, 7.5]	0.1	l_4 (m)	[1.5, 3.0]	0.1
t_1 (m)	[0.25, 0.5]	0.1	t_2 (m)	[0.3, 0.5]	0.1
t_3 (m)	[0.8, 1.6]	0.1	α_1	[2,30]	2
α_2	[10,20]	2			

assumed as 3000 local currency per ton.

V_c can be calculated from the cooling tower geometries defined in Fig. 9. THe steel reinforcement consumed for cooling tower should satisfy two requirement.

The first requirement is the material strength limit

$$\gamma_g S_{GK} + \gamma_w S_{WK_{WLP_i}} + \gamma_t S_{TK} \le R(\sigma_c, \sigma_f, M_s, \Gamma) \tag{10}$$

where S is the cooling tower design loads including self-weight GK, temperature loads TK, wind loads WK for considered ith wind load pattern (WLP_i); γ_g, γ_w and γ_t are the partially coefficients for self-weight, wind load and temperature loads, respectively; σ_c and σ_f is the design material ultimate stress for concrete and steel, respectively; M_s is the steel volume required, and Γ represents array of the cooling tower geometry variables in Fig. 9.

The second requirement is local buckling factor K_B should not be smaller than 5 ($K_B \ge 5$), and K_B is defined in Chinese design Code [40]:

$$0.8K_B\left(\frac{\sigma_1}{\sigma_{cr1}}+\frac{\sigma_2}{\sigma_{cr2}}\right)+0.2K_B^2\left[\left(\frac{\sigma_1}{\sigma_{cr1}}\right)^2+\left(\frac{\sigma_2}{\sigma_{cr2}}\right)^2\right]=1 \tag{11a}$$

$$\sigma_{cr1}=\frac{0.985E_c}{(1-\nu_c^2)^{3/4}}\left(\frac{t_2}{R_2}\right)^{4/3}K_1 \tag{11b}$$

$$\sigma_{cr2}=\frac{0.612E_c}{(1-\nu_c^2)^{3/4}}\left(\frac{t_2}{R_2}\right)^{4/3}K_2 \tag{11c}$$

in which σ_1 and σ_2 are the concrete stress under the self weight loading, winds loading and internal thermal pressure loading in the circumferential and meridian direction, respectively; σ_{cr1} and σ_{cr2} are concrete critical stress in the circumferential and meridian direction, respectively; ν_c is the Poisson's ratio of concrete; K_1 and K_2 is the geometrical parameters defined in Table 9.4.14 in Refs. [40].

3.1.4. Final crossover check for multiple WLPs

For each wind load pattern, based on the above optimization constraints and object, one set of cooling tower optimized structures (OS) geometry parameters can be found, and associated cost on construction material required is also calculated. However, it is still possible that the optimized structural design including cooling tower geometries and reinforcement volume may fail the material strength limit in Eq. (10) and local buckling requirement in Eq. (11) under other wind load patterns. Thus this study propose to crossover check the optimized structural design against other wind load patterns. At last, the optimized structural design with minimum construction cost, which also can pass the requirement of all wind load patterns will be selected as final optimized structural design. The process of crossover check is illustrated in Fig. 10.

3.2. Optimization algorithm: gradient descent based on grid search

The gradient descent algorithm is a classic mathematical optimization method, which is suitable for local minimum optimization. However, the cooling tower structural design shown in previous section is highly possible a multiple local minimum optimization problem, which require global optimization algorithm. In this study, a two-step grid search method is proposed to seek possible valleys containing minimum, then gradient descent algorithm is utilized to find the accurate minimum point.

In this section, an example of searching for the lowest elevation of Eggholder function in Eq. (12) in the domain of $x \in [0, 800]$, $y \in [1000, 1800]$ is given below to conceptually illustrate its optimization procedure.

$$f(x,y) = -(y+47)\sin\left(\sqrt{\left|y+\frac{x}{2}+47\right|}\right) - x\sin\left(\sqrt{|x-(y+47)|}\right) \tag{12}$$

The actual elevation of Eggholder function is plotted in Fig. 11, and, for illustration purpose, the z axis is plotted as negative direction upwards.

At the first round, the whole domain is divided into 8×8 grid as shown in Fig. 12, then, at the grid center, $f(x,y)$ is evaluated and ranked from lowest to highest. Next, 8 regions with lowest function values are selected into the second refined grid, which are plotted as colorful areas, and other regions are ruled out and plotted as gray-scale in Fig. 12.

At the second round, each selected refined region is further divided into 4×4. Similarly, at the center of refined region, $f(x,y)$ is evaluated, and the points with minimum value are selected as the start point of gradient descent.

Third, standard gradient descent algorithm is performed to find the local minimum near the selected start from previous two rounds grid search. Fig. 13 illustrate the minimum searching path by gradient descent from three starting points at the region $x \in [600, 800]$, $y \in [1600, 1800]$, and they all reach the same destinations. Finally, the several local minimums from the different starting points are compared, and the most minimum point will be found at last.

4. Optimization process and results

4.1. Cooling tower structural optimization for individual wind load pattern

The first wind load pattern (WLP1) about code-specified symmetrical

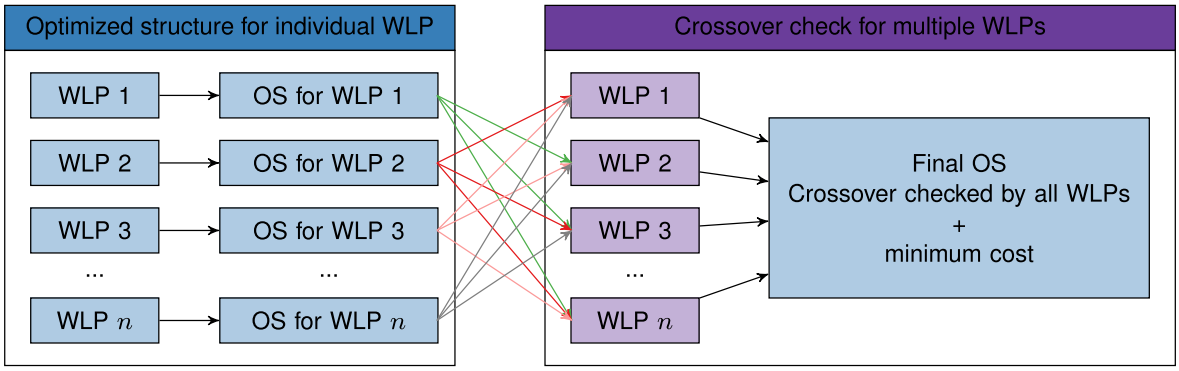

Fig. 10. Crossover check of optimized structures under multiple wind load patterns.

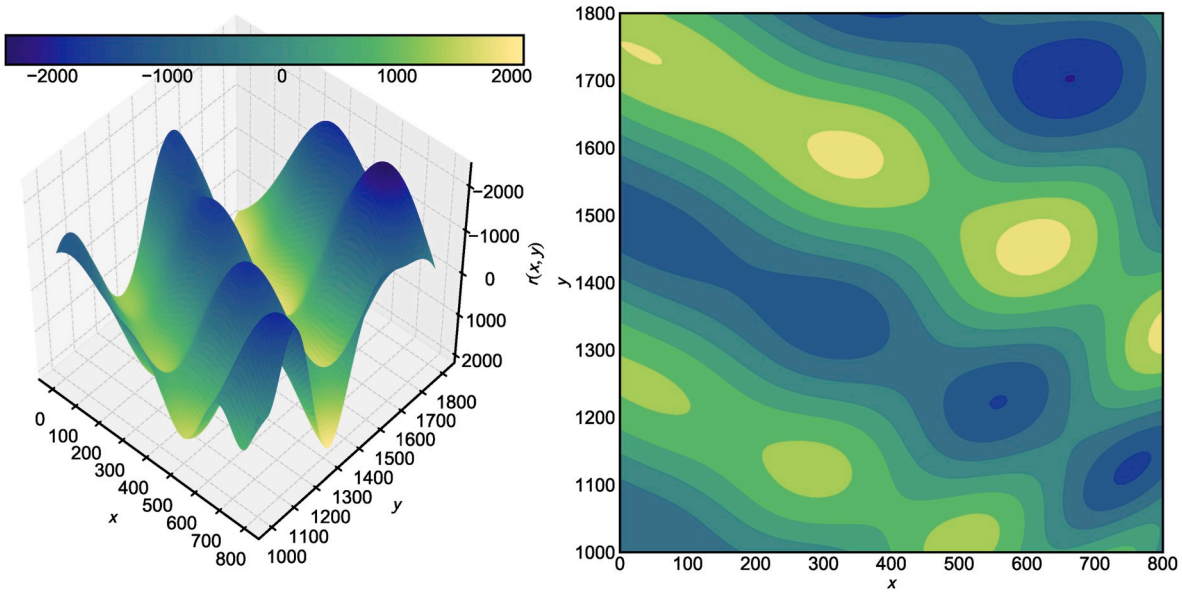

Fig. 11. Eggholder function at the region $x \in [0, 800], y \in [1000, 1800]$

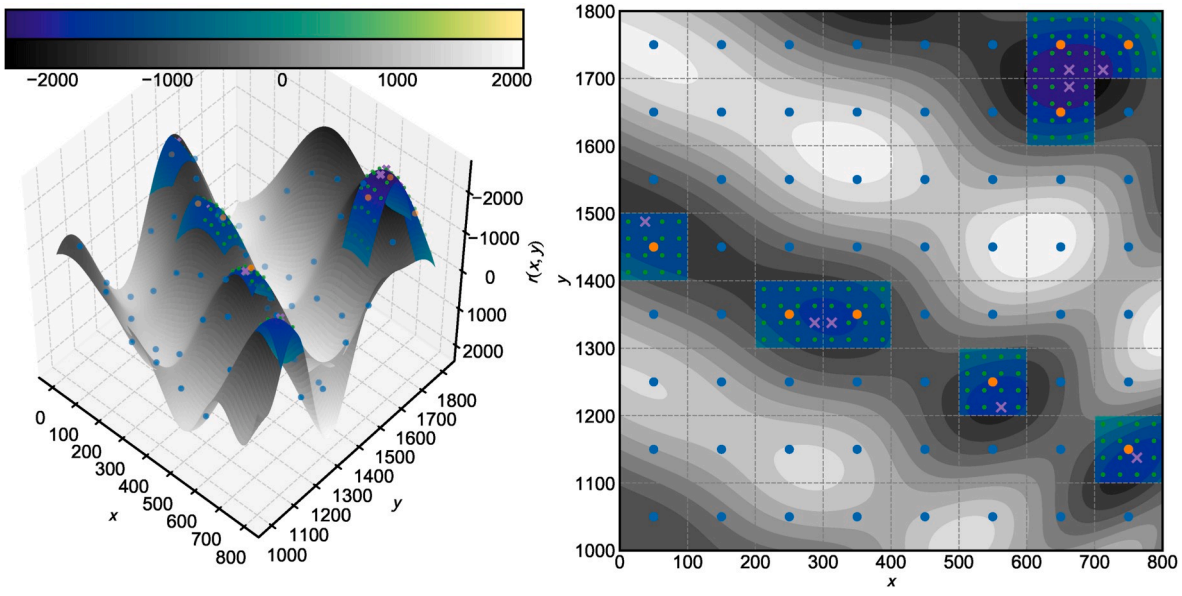

Fig. 12. Possible regions having minimum through grid search and refined grid search.

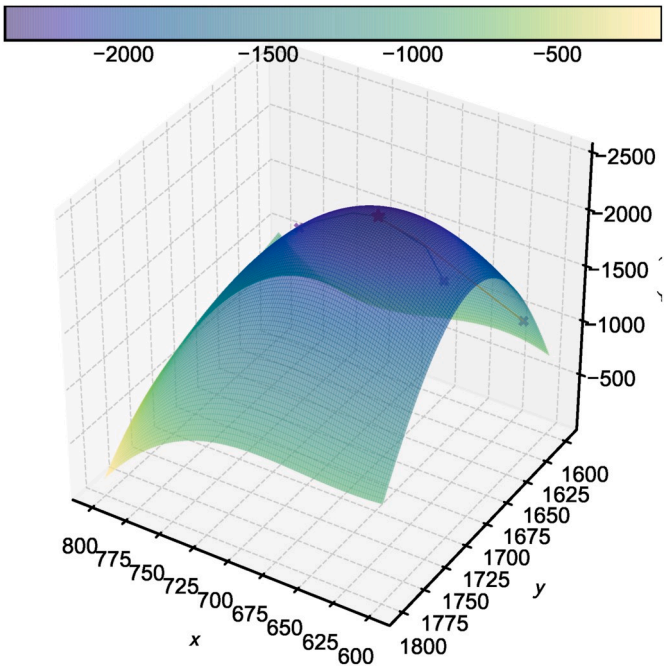

Fig. 13. Seeking Minimum through gradient descent.

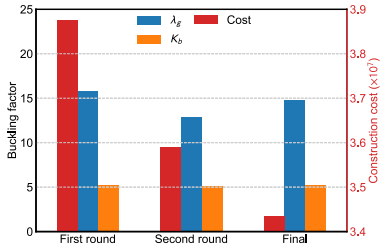

Fig. 14. Stability factors and construction cost at three optimization stages.

2-D wind load pattern for isolated tower is employed to show the optimization process. According to the optimization methods mentioned in previous section, the first round of grid search points is presented in Table 6. After comparing the cost from different cooling tower geometry parameters configuration, the minimum cost is 3.875×10^7 and the optimal parameters are also list in Table 6 (see Table 7).

The second round grid search is based on the results from the first round. There are three parameters (θ_1, d_1, d_2) already locate at the boundary of domain, therefore their values are fixed, and grid points of other parameters are refined. Similarly, comparing the construction cost of different parameters combination, the minimum cost is 3.59×10^7, which is reduced by 7.35%.

The optimal parameters set from second round grid search is used as the starting point for gradient descent, the new structural design parameters of cooling tower with minimum cost is list in Table 8. Comparing the second round grid search, most parameters stay the same, and only two parameters (l_1 and t_2) are slightly adjusted, and the final optimal construction cost is 3.434×10^7, which is reduced by 4.34%. The construction cost and global/local buckling factors are plotted in Fig. 14.

The cost can be reduced effectively at every stages. The global bucking factors λ largely exceed the design code limit 5 and the local buckling factor is slightly over than 5, which ensure the stability of cooling tower structure. For other three wind load patterns, the same procedure is applied and the optimal geometry parameters for each WLP is listed in Table 8. Corresponding to four kinds of wind load patterns, the optimized structural design is named as OS1, OS2, OS3 and OS4, respectively.

Table 6
First round of grid search points for cooling tower structural optimization.

Variables	Grid points	Optimal points	Variables	Grid points	Optimal points
θ_1 (°)	[7,8,9]	8	θ_2 (°)	[13,17,21]	21
d_1 (m)	[0.2, 0.4, 0.6]	0.6	d_2 (m)	[0.9, 1.2, 1.5]	0.9
l_1 (m)	[0.6, 0.9, 1.2]	0.9	l_2 (m)	[0.6, 0.9, 1.2]	0.9
l_3 (m)	[6.5, 7.0, 7.5]	7	l_4 (m)	[1.7, 2.3, 2.8]	2.3
t_1 (m)	[0.25, 0.35, 0.5]	0.35	t_2 (m)	[0.30, 0.33, 0.35]	0.33
t_3 (m)	[0.8, 1.2, 1.6]	1.2	α_1	[10,20,30]	30
α_2	[10,14,20]	14			

Table 7
Second round of grid search points for cooling tower structural optimization.

Variables	Grid points	Optimal points	Variables	Grid points	Optimal points
θ_1 (°)	8	8	θ_2 (°)	[18,19,20]	20
d_1 (m)	0.6	0.6	d_2 (m)	0.9	0.9
l_1 (m)	[0.8, 0.9, 1.0]	0.8	l_2 (m)	[0.8, 0.9, 1.0]	0.8
l_3 (m)	[6.9, 7.0, 7.1]	6.9	l_4 (m)	[1.9, 2.3, 2.7]	1.9
t_1 (m)	[0.30, 0.35, 0.4]	0.3	t_2 (m)	[0.32, 0.33, 0.34]	0.33
t_3 (m)	[1.0, 1.2, 1.4]	1.4	α_1	[26,28,30]	26
α_2	[13,14,15]	14			

4.2. Crossover check

Crossover check is designed to test and verify whether the initial OS from each particular wind load pattern can meet the requirement of other wind load patterns, and to further select the final optimized cooling tower structural design, which is suitable for all possible wind load patterns. Fig. 15 shows the global and local buckling factors of different optimized structures (OS) under four kinds of WLPs. It is obvious that different wind load patterns generate various geometry sizes, and a structure optimized for one certain WLP cannot necessarily stay safe under other WLPs.

Table 8
Final optimal parameters for cooling tower structural optimization.

Variables	WLP1	WLP2	WLP3	WLP4
θ_1 (°)	8	9	8	8
θ_2 (°)	20	20	20	20
d_1 (m)	0.6	0.6	0.6	0.6
d_2 (m)	0.9	0.9	0.9	0.9
l_1 (m)	0.7	0.6	0.7	0.7
l_2 (m)	0.8	0.8	0.8	0.8
l_3 (m)	6.9	6.1	6.4	6.7
l_4 (m)	1.9	1.7	2.1	1.7
t_1 (m)	0.3	0.25	0.25	0.25
t_2 (m)	0.35	0.33	0.34	0.35
t_3 (m)	1.4	1.2	1.4	1.2
α_1	26	10	26	2
α_2	14	12	14	10
C (10^7)	3.434	2.481	2.962	2.992

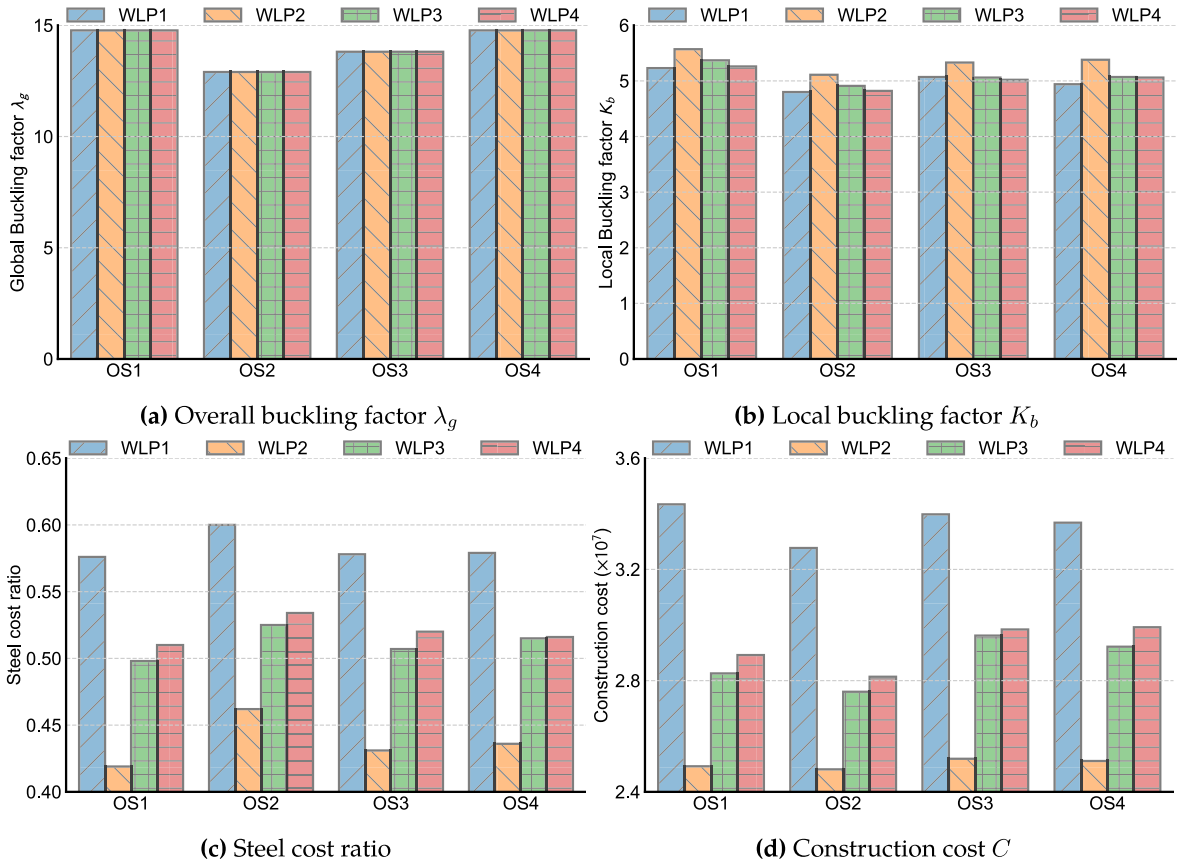

Fig. 15. Crossover comparison of individual optimization results.

Fig. 15a shows that global buckling factor is satisfied for OS1∼4 under all 4 WLPs. However, in Fig. 15b, local buckling factor limit is not fulfilled when OS2 is under other 3 wind load patterns and when OS4 is under WLP1, being less than the lower limit of 5.0 specified in the Chinese design Code [40]. Therefore, only OS1 and OS3 pass the crossover check from the aspect of structure stability. From the construction cost plots in Fig. 15d, OS1 has better generalization performance among four kinds of WLPs. Comparing with OS3, OS1 has lower cost for WLP2∼4, and OS1's cost on WLP1 is only slightly over than OS3. On the other hand, the global and local buckling factor of OS1 is higher than OS3. Thus, the OS1 is selected as the final optimal structural design geometry.

Steel Reinforcement ratio along cooling tower height of the final selected OS1 is plotted in Fig. 16. It is obvious that steel consumption depends on wind load patterns. Generally, reinforcement under the wind load patterns specified by Codes tends to be conservative. Under C–S-2D (WLP1), reinforcements outside and inside the tower meridian are greater at most shell elevations than those under other patterns; circumferential reinforcement is also not less than those of the other wind load patterns. However, it cannot be ignored since local failure can lead to global destruction. The relation among reinforcement curves under different wind load patterns varies respectively in the top and bottom parts, which reflect obvious 3-D effect near cooling tower top and ground.

5. Conclusions

Typical adverse wind load patterns (WLPs) of grouped cooling towers are proposed in this study as the evaluation criteria of structural overall design. Furthermore, structural construction cost optimization, which involves optimization for individual WLP and crossover check among four WLPs, is implemented through nested grid search and gradient descent method. In this optimization process, construction cost including concrete and steel consumption is utilized as the optimization target and geometry constraints to ensure the cooling performance and structural stability constraints against buckling are also applied.

5.1. Main conclusions are summarized as follows

1. Typical adverse wind load patterns for cooling tower with rhombus arrangements are more serious than rectangle arrangement due to the asymmetry amplification. The major interference for rectangle arranged towers is "shelter effect" and, for rectangle arranged towers, "funneling" is the significant interference effect.
2. Overall optimization design of large cooling towers is valuable and necessary for both structure safety and economic efficiency. The hybrid optimization algorithm of the grid search and gradient seeking method is an efficient algorithm than traditional experience-based design method.
3. Structure optimization greatly depends on wind load patterns and some optimized parameters greatly change under different wind load patterns.
4. Through individual optimization and crossover check, a final optimized structure considering the both superstructure and substructures can meet multiple requirements of structure safety, stability and economic efficiency.

Declaration of competing interests

The authors declare that they have no known competing financial interests or personal relationships that could have appeared to influence the work reported in this paper.

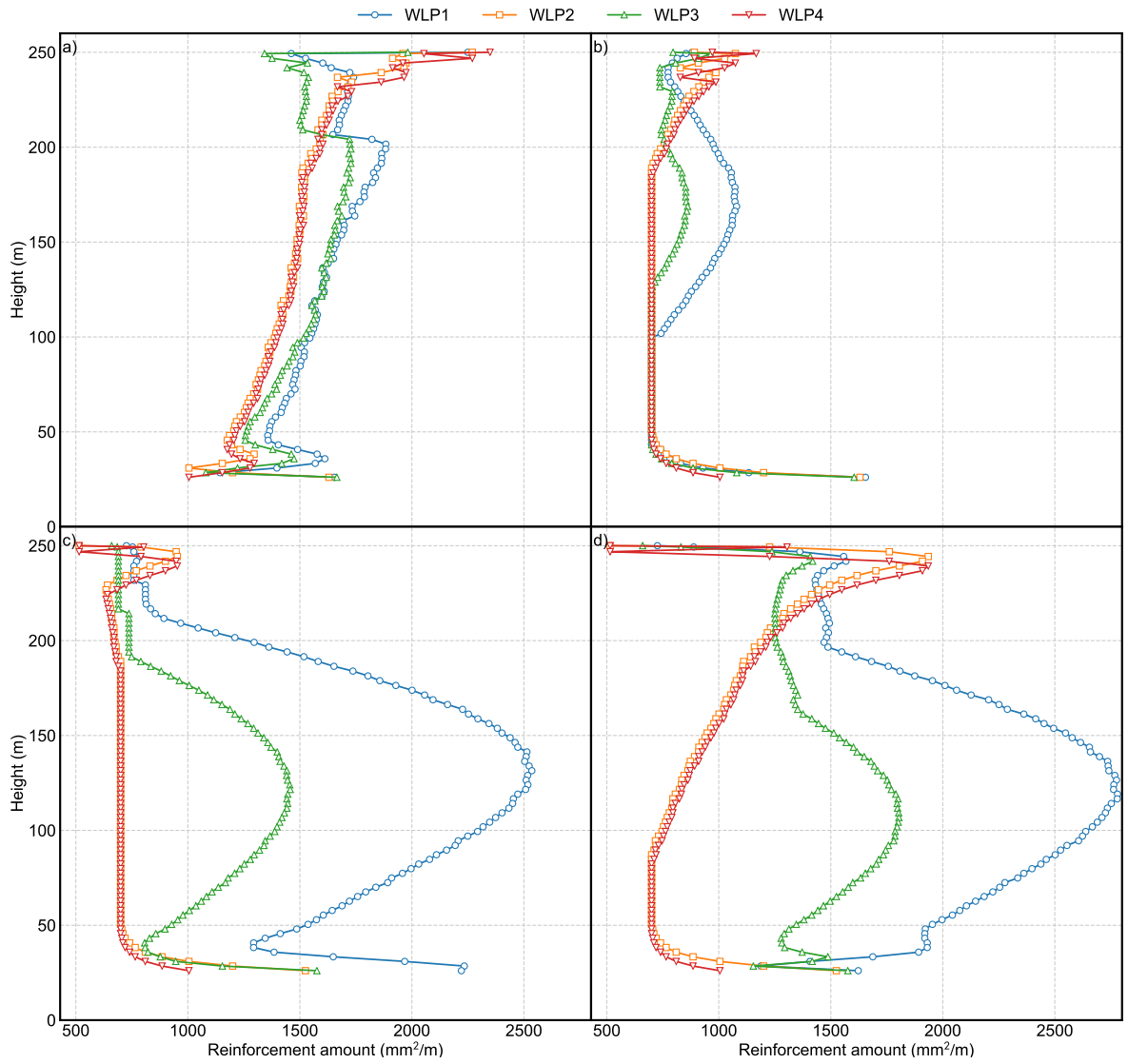

Fig. 16. Reinforcement amount of optimal structural design under 4 WLPs (a, Outside along circumference; b, Inside along circumference; c, Outside along meridian; d, Inside along meridian).

CRediT authorship contribution statement

Lin Zhao: Conceptualization, Methodology, Writing - review & editing. **Wei Cui:** Data curation, Visualization, Writing - original draft. **Yanyan Zhan:** Validation. **Zhinan Wang:** Software. **Yuwen Liang:** Investigation. **Yaojun Ge:** Supervision.

Acknowledgments

The authors gratefully acknowledge the support of the National Key Research and Development Program of China (2018YFC0809600, 2018YFC0809604), the National Natural Science Foundation of China (51678451) and Shanghai Pujiang Plan (No. 19PJ1409800). Any opinions, findings and conclusions or recommendations are those of the authors and do not necessarily reflect the views of either the NSFC or any other sponsors.

Appendix A. Supplementary data

Supplementary data to this article can be found online at https://doi.org/10.1016/j.tws.2020.106740.

References

[1] W. Li, J. Chai, J. Zheng, Investigation of natural draft cooling tower in China, Heat Tran. Eng. 38 (11–12) (2017) 1101–1107.
[2] D. Busch, R. Harte, W.B. Krätzig, U. Montag, New natural draft cooling tower of 200 m of height, Eng. Struct. 24 (12) (2002) 1509–1521.
[3] A. Zingoni, Structural health monitoring, damage detection and long-term performance, Eng. Struct. 12 (27) (2005) 1713–1714.
[4] P. Bamu, A. Zingoni, Damage, deterioration and the long-term structural performance of cooling-tower shells: a survey of developments over the past 50 years, Eng. Struct. 27 (12) (2005) 1794–1800.
[5] W. Cui, L. Caracoglia, Simulation and analysis of intervention costs due to wind-induced damage on tall buildings, Eng. Struct. 87 (2015) 183–197.
[6] W. Cui, L. Caracoglia, A unified framework for performance-based wind engineering of tall buildings in hurricane-prone regions based on lifetime intervention-cost estimation, Struct. Saf. 73 (2018) 75–86.
[7] H.J. Niemann, H. Pröpper, Some properties of fluctuating wind pressures on a full-scale cooling tower, J. Wind Eng. Ind. Aerod. 1 (1975) 349–359.
[8] H.J. Niemann, Wind effects on cooling-tower shells, J. Struct. Div. 106 (3) (1980) 643–661.
[9] H.J. Niemann, J. Ruhwedel, Full-scale and model tests on wind-induced, static and dynamic stresses in cooling tower shells, Eng. Struct. 2 (2) (1980) 81–89.
[10] H.J. Niemann, W. Zerna, Impact of research on development of large cooling towers, Eng. Struct. 8 (2) (1986) 74–86.
[11] H.J. Niemann, H.D. Köpper, Influence of adjacent buildings on wind effects on cooling towers, Eng. Struct. 10 (20) (1998) 874–880.
[12] Tf Sun, Lm Zhou, Wind pressure distribution around a ribless hyperbolic cooling tower, J. Wind Eng. Ind. Aerod. 14 (1–3) (1983) 181–192.

[13] T. Sun, Z. Gu, L. Zhou, P. Li, G. Cai, Full-scale measurement and wind-tunnel testing of wind loading on two neighboring cooling towers, J. Wind Eng. Ind. Aerod. 43 (1–3) (1992) 2213–2224.
[14] L. Zhao, Y. Ge, A. Kareem, Fluctuating wind pressure distribution around full-scale cooling towers, J. Wind Eng. Ind. Aerod. 165 (2017) 34–45.
[15] L. Zhao, X. Chen, S. Ke, Y. Ge, Aerodynamic and aero-elastic performances of super-large cooling towers, Wind Struct. 19 (4) (2014) 443–465.
[16] L. Zhao, X. Chen, Y. Ge, Investigations of adverse wind loads on a large cooling tower for the six-tower combination, Appl. Therm. Eng. 105 (2016) 988–999.
[17] R. Pope, Structural deficiencies of natural draught cooling towers at UK power stations. part 1: failures at ferrybridge and fiddlers ferry, Proceedings of the Institution of Civil Engineers Structures and Buildings 104 (1) (1994) 1–10.
[18] L. Zhao, Y. Zhan, Y. Ge, Wind-induced equivalent static interference criteria and its effects on cooling towers with complex arrangements, Eng. Struct. 172 (2018) 141–153.
[19] M. Yu, L. Zhao, Y. Zhan, W. Cui, Y. Ge, Wind-resistant design and safety evaluation of cooling towers by reinforcement area criterion, Eng. Struct. 193 (2019) 281–294.
[20] Code of Practice for Structural Design and Construction, Part 4: Water Cooling Towers, BSI-Bs4485-4:1996, British Standards Institution, London, United Kingdom, 1996.
[21] Structural Design of Cooling Towers, Essen, Germany, 2005. VGB-R 610Ue:2005, VGB PowerTech. E.V.
[22] Code for Hydraulic Design of Fossil Fuel Power Plants, China Planning Press, Beijing, China, 2014. GB50102T:2014.
[23] R. Harte, W. Krätzig, Large-scale cooling towers as part of an efficient and cleaner energy generating technology, Thin-Walled Struct. 40 (7–8) (2002) 651–664.
[24] J. Form, The ring-stiffened shell of the ISAR II nuclear power plant natural-draught cooling tower, Eng. Struct. 8 (3) (1986) 199–207.
[25] S. Sabouri-Ghomi, M.H.K. Kharrazi, P. Javidan, Effect of stiffening rings on buckling stability of RC hyperbolic cooling towers, Thin-Walled Struct. 44 (2) (2006) 152–158.
[26] I. Mungan, O. Lehmkamper, Buckling of stiffened hyperboloidal cooling towers, J. Struct. Div. 105 (10) (1979) 1999–2007.
[27] W. Böhm, Untersuchungen zur technisch-ökonomischen auslegung und bewertung von naturzug-kühltümen, Diplomarbeit, Technische Universität Dresden, Dresden, Germany, 1969.
[28] J. Croll, The influence of shape on the stresses in cooling towers, Proc. Inst. Civ. Eng. 42 (3) (1969) 383–396.
[29] R. Mclone, Effect of loading on cooling towers of three different shapes, Conc. Const. Eng. 58 (8) (1963).
[30] D.A.W. Greiner-Mai, Beitrag zur entscheidungsfindung beim entwurf hyperbolischer kühltürme mit besonderer breücksichtigung des statisch-konstruktiven aspekts, Diplomarbeit, IAB – Institut für Angewandte Bauforschung Weimar gGmbH, Weimar, Germany, 1973.
[31] H.C. Noh, Nonlinear behavior and ultimate load bearing capacity of reinforced concrete natural draught cooling tower shell, Eng. Struct. 28 (3) (2006) 399–410.
[32] S.M. Spence, M. Gioffrè, Large scale reliability-based design optimization of wind excited tall buildings, Probabilist. Eng. Mech. 28 (2012) 206–215.
[33] Y. Li, Q.S. Li, Wind-induced response based optimal design of irregular shaped tall buildings, J. Wind Eng. Ind. Aerod. 155 (2016) 197–207.
[34] J. Croll, Recommendations for the design of hyperbolic or other similarly shaped cooling towers, in: Proceedings of Internation Assoction for Shell and Spatial Structures Working Group, 1971.
[35] H. Uysal, R. Gul, U. Uzman, Optimum shape design of shell structures, Eng. Struct. 29 (1) (2007) 80–87.
[36] N.D. Lagaros, V. Papadopoulos, Optimum design of shell structures with random geometric, material and thickness imperfections, Int. J. Solid Struct. 43 (22–23) (2006) 6948–6964.
[37] S. Gupta, C. Manohar, An improved response surface method for the determination of failure probability and importance measures, Struct. Saf. 26 (2) (2004) 123–139.
[38] M.J. Tahk, H.W. Woo, M.S. Park, A hybrid optimization method of evolutionary and gradient search, Eng. Optim. 39 (1) (2007) 87–104.
[39] N.J. Sollenberger, D.P. Billington, R.H. Scanlan, Wind loading and response of cooling towers, J. Struct. Div. 106 (3) (1980) 601–621.
[40] Technical Specification for Hydraulic Design of Thermal Power Plants, National Energy Administration of China, Beijing, China, 2018. DL/T5339:2018.